Geodetic slip model of the 2011 M9.0 Tohoku earthquake

Fred F. Pollitz,[1] Roland Bürgmann,[2] and Paramesh Banerjee[3]

Received 27 June 2011; revised 26 July 2011; accepted 28 July 2011; published 1 September 2011.

[1] The three-dimensional crustal displacement field as sampled by GPS is used to determine the coseismic slip of the 2011 M9.0 Tohoku Earthquake. We employ a spherically layered Earth structure and use a combination of onland GPS, out to ~4000 km from the rupture, and offshore GPS, which samples the high-slip region on the interplate boundary along the Japan trench. Inversion of the displacement field for dip slip, assuming an interplate boundary of variable dip and striking 195°, yields a compact slip maximum of about 33 m located 200 km east of Sendai. The geodetic moment is 4.06×10^{22} N m, corresponding to $M_w = 9.0$. The area of maximum slip is concentrated at a depth of about 10 km, is updip of the rupture areas of the $M \gtrsim 7$ Miyagi-oki earthquakes of 1933, 1936, 1937, and 1978, and roughly coincides with the rupture area of the M7.1 1981 Miyagi-oki earthquake. The overlap of the 2011 slip area with several preceding ruptures suggests that the same asperities may rupture repeatedly with $M \gtrsim 7$ events within several decades of one another. **Citation:** Pollitz, F. F., R. Bürgmann, and P. Banerjee (2011), Geodetic slip model of the 2011 M9.0 Tohoku earthquake, *Geophys. Res. Lett.*, *38*, L00G08, doi:10.1029/2011GL048632.

1. Introduction

[2] The March 11, 2011 M9.0 Tohoku Earthquake resulted from dip slip on the Japan trench accommodating ~8 cm/yr convergence between the Pacific and Okhotsk plates [*Seno et al.*, 1996] (Figure 1a). Over the past 100 years the interplate boundary of northeast Japan has had numerous smaller ruptures up to magnitude ~7.5. Large areas of high locking on the interplate boundary east of Miyagi have been recognized [e.g., *Nishimura et al.*, 2000; *Suwa et al.*, 2006; *Hashimoto et al.*, 2009; *Loveless and Meade*, 2010; *Sato et al.*, 2011b], while the area to the south of ~37°N has exhibited numerous small repeating events that indicate widespread aseismic fault slip on the megathrust in that area [*Uchida et al.*, 2009; *Uchida and Matsuzawa*, 2011]. It is important to understand the relation of the slip areas of the preceding earthquake ruptures to the slip distribution of the 2011 M9.0 event, as well as to understand the cycle of strain accumulation and release in light of the 2011 event.

[3] Slip inversions utilizing long-period seismic data, tsunami waveform height data, and crustal displacement data from Japanese onshore GPS [*Hayes*, 2011; *Simons et al.*, 2011; *Lay et al.*, 2011; *Koper et al.*, 2011] (ERI, 2011, available at http://outreach.eri.u-tokyo.ac.jp/eqvolc/201103_tohoku/; G. Shao et al., 2011, available at http://www.geol.ucsb.edu/faculty/ji/big_earthquakes/2011/03/0311/Honshu_main.html) yield a compact rupture with a large (~45–60 m) slip maximum at depth $\lesssim$ 10 km. Although these distributions have been demonstrated to be consistent with the Japanese onland GPS network data (GEONET), questions arise as to the robustness of the obtained slip inversions, e.g., kinematic broadband slip inversions may yield slip distributions very different from those obtained with combined tsunami and GPS datasets [*Simons et al.*, 2011] or from short-period seismic data [*Koper et al.*, 2011]. Recent geodetic slip inversions using onland data from GEONET [*Ozawa et al.*, 2011] or from GEONET and Tohoku University [*Iinuma et al.*, 2011] also fit the onland GPS very well but differ in the details of their respective slip distributions. Important issues are whether geodetic data alone demands the same slip pattern as seismic and tsunami waveform height data, what constraints are added by offshore GPS data, and to what level of detail the available slip models can explain both the near-field and far-field crustal displacement field.

[4] In this study we use a comprehensive GPS data set in order to derive a geodetic slip model. It covers a wide spectrum of spatial scales of deformation, from the offshore area directly above the high-slip region to the far field extending ~4000 km from the rupture.

2. Data Set

[5] Data from the Geospatial Information Authority (GSI) of Japan was processed by the U.S. Jet Propulsion Laboratory (JPL) (ftp://sideshow.jpl.nasa.gov/pub/usrs/ARIA) to yield the three-dimensional coseismic displacement field over the Japanese Islands (yellow vectors in Figure 2 and Figure S1 in the auxiliary material).[1] This displacement field is based on observations made from six minutes preceding to nine minutes after the mainshock origin time. The standard deviation in three-dimensional displacement is ~1–5 cm throughout the area.

[6] In the offshore region, seafloor precision acoustic transponders off Miyagi Prefecture combined with shipboard GPS yield the three-dimensional coseismic displacement field at five offshore locations (green vectors in Figures 2 and S1) [*Sato et al.*, 2011a]. These measurements are based on a post-earthquake observation time of March 28–29, 2011 and may therefore contain some signal from 17 days of afterslip. The standard deviation is about 0.25 m.

[7] In the far field, data from the International GPS Service (IGS) were processed with the GAMIT/GLOBK 10.4 software package [*Herring et al.*, 2010] to produce time series of station coordinates in the ITRF-2005 reference frame spanning at least 20 days before and after the earthquake. We

[1]U.S. Geological Survey, Menlo Park, California, USA.
[2]Department of Earth and Planetary Sciences, University of California, Berkeley, California, USA.
[3]Earth Observatory of Singapore, Nanyang Technological University, Singapore.

0094-8276/11/2011GL048632

[1]Auxiliary materials are available in the HTML. doi:10.1029/2011GL048632.

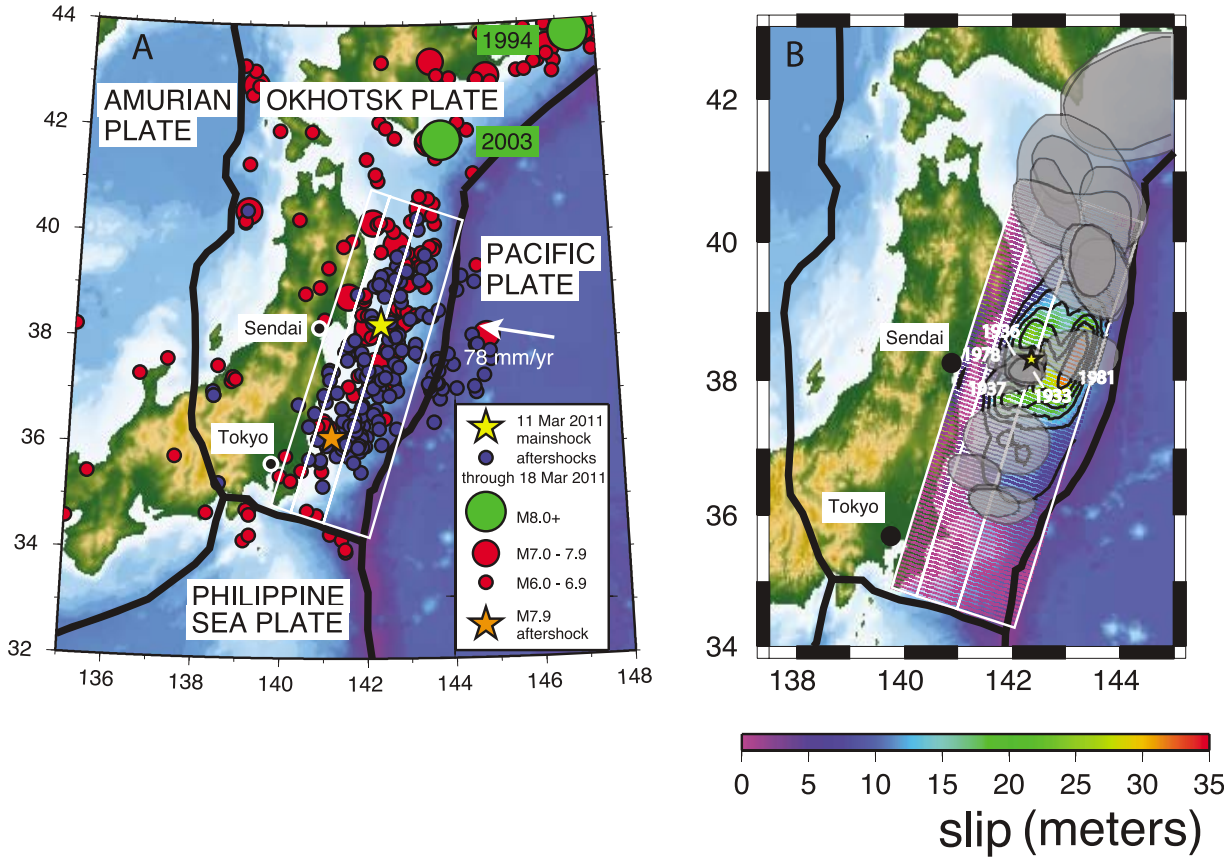

Figure 1. (a) Historic earthquakes and aftershocks of the March 11, 2011 event. Historical epicenters (1973-2011) and aftershock locations are provided by the National Earthquake Information Center. White lines indicate the surface projection of the variable-dip fault planes used to model the 2011 event. Pacific - Okhotsk relative plate motion vector is from *Apel et al.* [2006]. (b) Slip distribution of the 2011 M9.0 Tohoku Earthquake assuming pure dip slip. Rupture areas of large interplate earthquakes from 1926 to 2008 [*Uchida et al.*, 2009] are superimposed in gray. Labels indicate the rupture areas of the 1933 M7.1, 1936 M7.4, 1937 M7.1, 1978 M7.4, and 1981 M7.1 Miyagi-oki earthquakes. A larger version of Figure 1 appears as Figure S8.

estimated offsets at the time of the earthquake by differencing the mean positions in the 5 days before and after the earthquake, respectively. The resulting horizontal displacement field is shown in Figure 3.

[8] The displacement field reveals that the coast of northeast Japan moved eastward up to 5 m, and the coastline generally subsided by about 0.5 m (up to a maximum of 1.1 m in eastern Miyagi Prefecture), presumably due to the position of the coast approximately above the lower edge of the rupture area along the interplate boundary. The seafloor of the overthrusting plate at the easternmost site (MYGI) moved east-southeastward up to a maximum of 24 m, with a corresponding uplift of 3 m. The crust at distances as far as 3000 to 4000 km from the rupture moved by ~3–5 mm.

3. Methods

[9] The fault geometry is that of three connected 700-km-long planar surfaces striking 195° (Figure 1a). The upper and lower edge depths are fixed at 3 km and 57 km, respectively. The dip is progressively steeper with greater depth: 10° from 3 to 21 km, 14° from 21 to 39 km, and 22° from 39 to 57 km depth. This geometry is consistent with the Global CMT solution and is similar to that adopted in recent seismic slip inversions. The location of the fault plane is guided by the slab contours of *Huang et al.* [2011]. The dip is thought to become progressively steeper from the trench towards land, where it may be 23° [*Miura et al.*, 2005].

[10] Experiments with spatially variable rake indicate that marginal improvement is gained by the inclusion of strike-slip components, and we therefore assume pure dip slip. Distributed dip slip on the fault plane is represented with a distribution of continuous functions as employed by *Pollitz et al.* [1998]. These are Hermite-Gauss (HG) functions of position on the rectangular fault plane. Slip on the slab interface is related to static surface displacement using the source response functions calculated with the method of *Pollitz* [1996]. This yields theoretical displacements in a layered spherical model with a spherical harmonic expansion. Global Earth model PREM with isotropic elastic parameters, appended by crustal structure appropriate for the offshore region of northeast Japan [*Zhao et al.*, 2007], is used for this purpose (Figure S2).

[11] Horizontal and vertical GPS data are inverted for distributed slip using weighted least squares. A small amount of damping of the squared gradient of the slip is used to regularize the inversion and determine the weighting coefficients of the HG functions [*Pollitz et al.*, 1998]. In these inversions, data from four IGS sites on Honshu (green vectors in Figure 3) are not used. The reason is that these data include

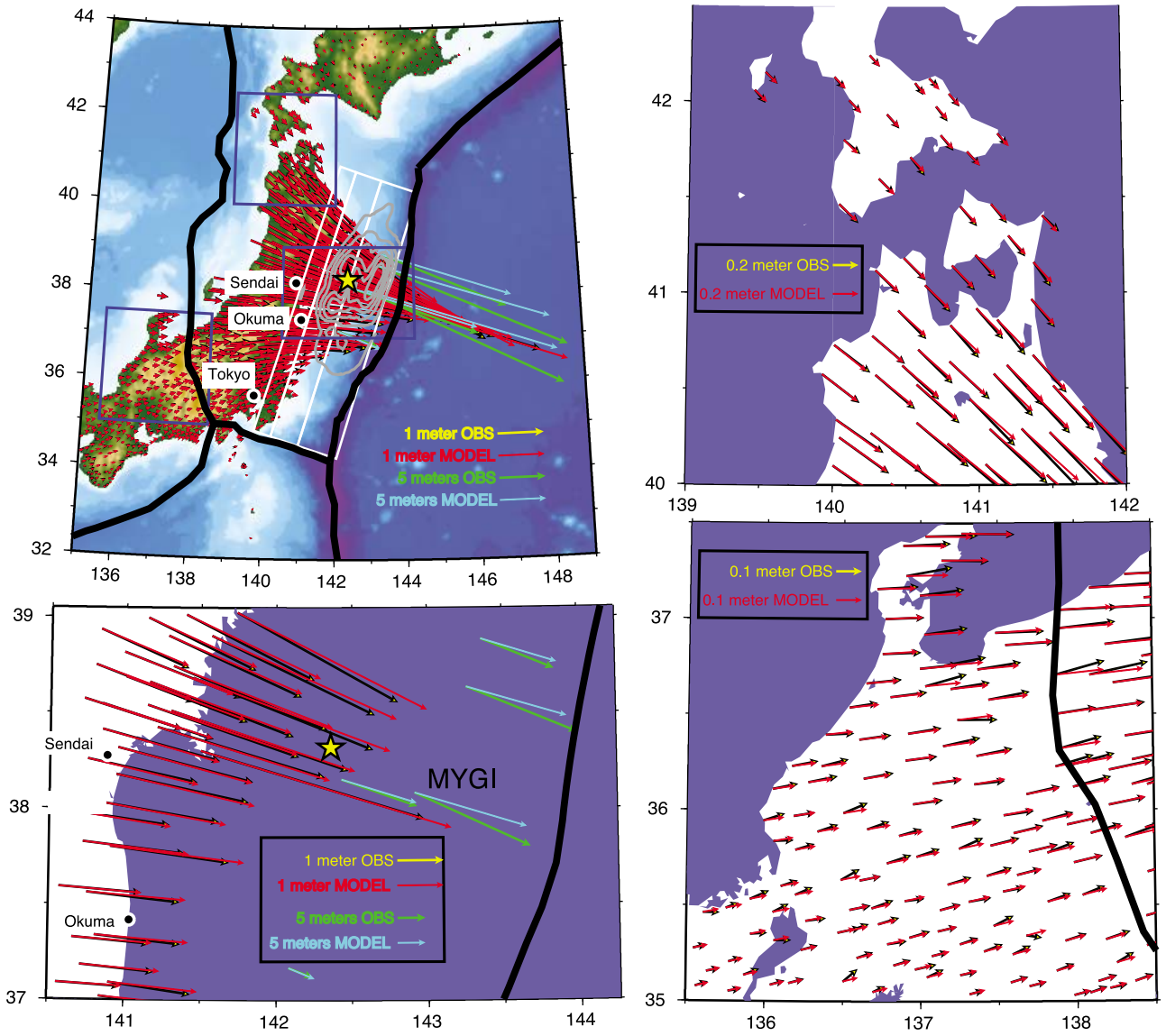

Figure 2. Observed ARIA v0.3 horizontal displacement field (yellow) vectors) and corresponding fit of the layered spherical model (red vectors), and observed GPS-A horizontal displacements (green vectors) and corresponding fit of the layered spherical model (blue vectors). Gray contours denote the fault slip in intervals of 5 m; the maximum slip is 33 m.

displacements from a large (M7.9) aftershock that occurred 30 minutes after the mainshock, whereas the GSI/ARIA-processed dataset does not include these displacements. Thus our results are intended to be representative of the mainshock exclusive of this large aftershock.

4. Results

[12] The resulting slip distribution is shown in Figure 1b, corresponding to a 'geodetic' moment of 4.06×10^{22} N m. Slip is concentrated directly updip of the CGMT hypocenter. Corresponding model fits to the horizontal and vertical GPS data are shown in Figures 2, 3, and S1.

[13] The importance of the offshore GPS data is shown in Figure S3, which presents alternative inversion results. Comparing parts (a) and (b) which use all data and only land data, respectively, slip inversions which do not account for the offshore GPS tend to localize the slip at greater depth along the interplate boundary and thus cannot adequately discriminate relatively deep slip from shallow slip. Moreover, the amount of slip required to fit the horizontal displacement field is substantially reduced when the locus of slip is deeper.

[14] The influence of layering in elastic structure is illustrated by comparing the slip distributions and model predictions of the spherically layered structure and a homogeneous sphere (with shear modulus of 40 GPa and Poisson's ratio of 0.25). The inversion results on the homogeneous sphere are presented in Figures S3c, S4, S5, and S6. Comparing Figures S3a and S3c, the slip distributions are similar, though the seismic moment is reduced by about 15% when using a homogeneous sphere. The homogeneous spherical model satisfactorily fits observed near-field displacements but systematically overpredicts the amplitude of far-field displacements (Figure S6). In contrast, the layered spherical model satisfactorily fits the amplitude of the horizontal displacement field at both near-field and far-field distances (Figures 2

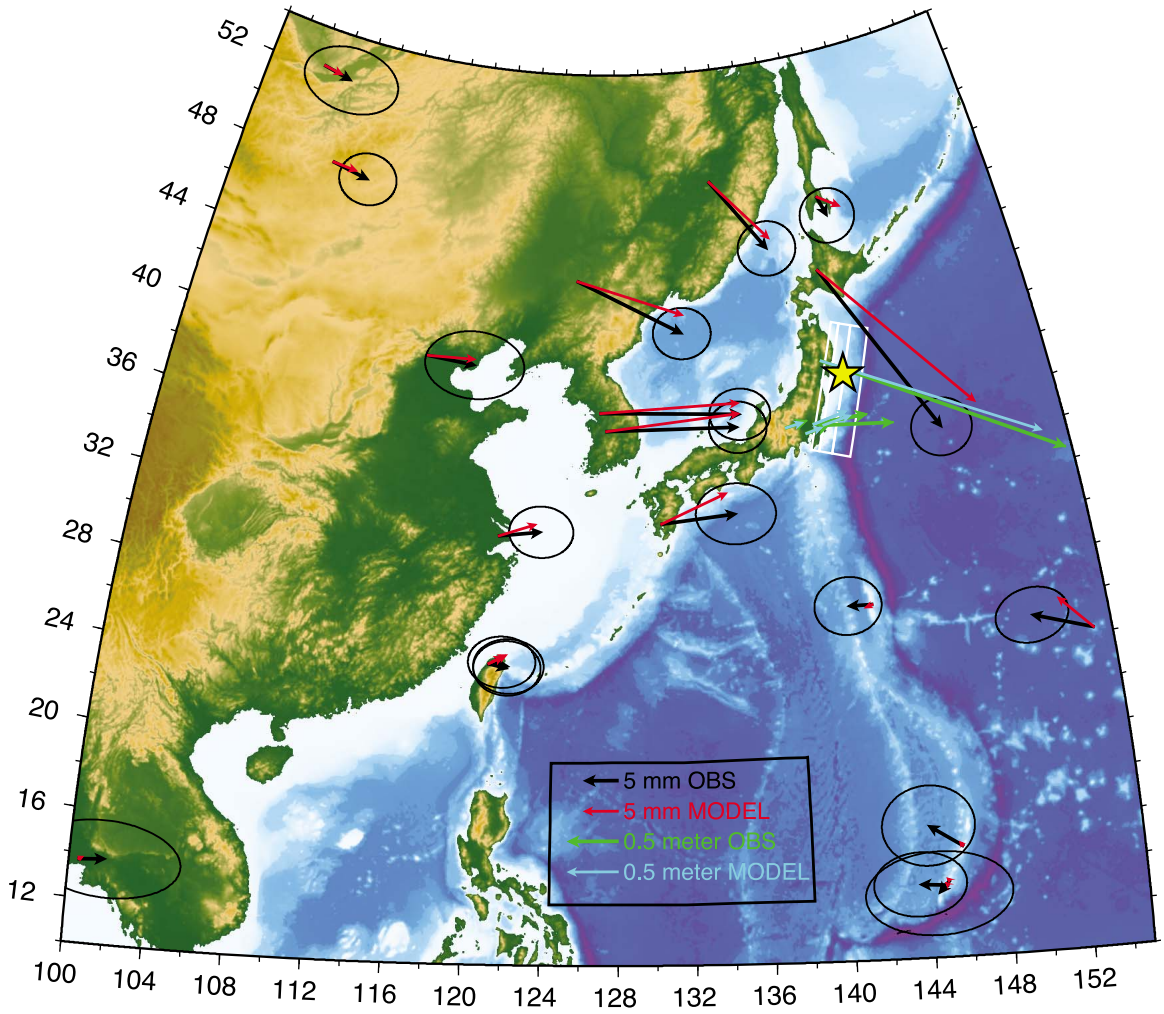

Figure 3. Observed horizontal displacement field at IGS sites (black and green vectors), plotted with 95% error ellipses, and corresponding fits of the layered spherical model (red and blue vectors).

and 3). This drawback of the homogeneous spherical model (and similarly the homogeneous half-space) has been previously illustrated for the 2004 Sumatra earthquake [*Banerjee et al.*, 2007] and 2010 Chile earthquake [*Pollitz et al.*, 2011].

[15] The slip maximum offshore Sendai is compact considering the earthquake size: the length of rupture exceeding 10 m is about 250 km. This is adjacent to the areas of peak ground acceleration onland (http://outreach.eri-u.tokyo.ac.jp/eqvolc/201103_tohoku/eng/). The high-slip region partially coincides with the location of high seismic coupling inferred from interseismic crustal velocity measurements [e.g., *Nishimura et al.*, 2000; *Suwa et al.*, 2006; *Hashimoto et al.*, 2009; *Loveless and Meade*, 2010], but it is generally well updip of the highly coupled area inferred in these studies. Our high-slip region generally coincides with the very shallow high-slip regions imaged in seismic studies [e.g., *Hayes*, 2011; *Simons et al.*, 2011; *Lay et al.*, 2011; *Koper et al.*, 2011] (http://outreach.eri.u-tokyo.ac.jp/eqvolc/201103_tohoku/; http://www.geol.ucsb.edu/faculty/ji/big_earthquakes/2011/03/0311/Honshu_main.html) and *Iinuma et al.*'s [2011] geodetic study.

[16] Preceding rupture areas of large interplate earthquakes during the past 85 years are shown together with the coseismic slip distribution in Figure 1b [*Uchida et al.*, 2009]. These historical ruptures tend to be located in the high-coupling zone [*Hashimoto et al.*, 2009]. They are generally proximal to the 2011 slip zone, except for some overlap with the Miyagi-oki ruptures in the 1930s and 1978 [*Yamanaka and Kikuchi*, 2004; *Umino et al.*, 2006], which are located downdip of the maximum coseismic slip area. The maximum slip region appears to coincide with the M7.1 1981 Miyagi-oki earthquake [*Yamanaka and Kikuchi*, 2004] (Figure 1b). The partial overlap of the historical and 2011 ruptures confirms the suggestions of *Okada et al.* [2005] and *Umino et al.* [2006] that the same asperities may rupture repeatedly in $M \gtrsim 7$ events within a few decades, including their collective rupture in an infrequent M9 event. As noted by *Iinuma et al.* [2011], the amount of 2011 slip at the location of the 1978 event is much larger than would have accumulated during the intervening 33 years, suggesting that preceding events did not involve complete stress drops.

[17] Resolution tests using simple synthetic input slip distributions (Figures S7a and S7c) indicate that lateral variations in slip are resolved at most depths, except for the southeasternmost corner of the imaged area (Figures S7b and S7d). At relatively shallow depth, slip is best resolved in the

northeastern portion of the imaged area because of the offshore GPS measurements of coseismic displacement.

5. Discussion

[18] Inversions based on seismic waveform inversions, with and without augmentation by GPS and tsunami wave height data [e.g., *Simons et al.*, 2011] yield a slip maximum up-dip of the hypocenter of order 50 m. This exceeds the maximum 33 m determined in this study using GPS data alone. We note that the observed 24 m displacement of the seafloor located above the subducted slab at ~10 km depth demands only ~33 m slip because of the presence of the free surface, i.e., with this geometry the hanging wall is expected to have an absolute displacement of about 75% of the fault slip and the footwall about 25% of the fault slip in the opposite direction.

[19] Numerous small repeating earthquakes have occurred along the Japan Trench along the entire area between ~35.5°N and 38°N, most intensely south of about 37°N [*Uchida et al.*, 2009]. Repeating earthquakes are generally found to represent small seismic asperities driven to repeated failure by aseismic slip on the surrounding fault plane [*Nadeau and McEvilly*, 1999]. The rapid decrease of coseismic slip south of this latitude (Figure 1b) suggests that either this region had lower levels of stored stress, thereby inhibiting rupture propagation, or that its frictional properties are different. The overall correlation of Tohoku-earthquake slip with the inferred distribution of interplate coupling [*Uchida and Matsuzawa*, 2011] would support both interpretations, since much of the long-term slip rate is presumably accommodated by aseismic creep in the areas of low effective coupling. In any case, postseismic GPS observations suggest that the area that produces repeating earthquakes has also experienced afterslip of order 1 m in the days following the Tohoku mainshock [*Ozawa et al.*, 2011].

[20] The coast of northeast Japan is generally subsiding during the interseismic interval [e.g., *Aoki and Scholz*, 2003; *Suwa et al.*, 2006], and this is rationalized with a 50-60 km depth of strong locking of the interplate boundary, a transition zone extending down to ~100 km depth [*Suwa et al.*, 2006]. Since the coastal region has undergone late Quaternary uplift [*Suzuki*, 1989; *Matsu'ura et al.*, 2009], interseismic subsidence is expected to be counteracted by coseismic uplift associated with megathrust earthquakes. However, the 2011 Tohoku event produced subsidence of the coast (Figure S1). This may be explained by the concentration of earthquake slip at relatively shallow depth <35 km. The peculiar situation that coseismic subsidence tends to reinforce interseismic subsidence in northeast Japan has been discussed by *Heki* [2007], who proposed that deep afterslip commonly follows large interplate ruptures. The 1978 M7.4 Miyagi-oki earthquake ruptured deeper (to ~50 km depth); it produced small coseismic subsidence of the coast but postseismic uplift likely due to deeper afterslip [*Ueda et al.*, 2001]. This raises the question as to how much of the interplate boundary deeper than the lower rupture limit of the 2011 Tohoku-oki event (~35 km) is highly coupled. It is noteworthy that the Kuril trench off Hokkaido exhibits a similar phenomenon, and there it has been inferred from geologic observations that large megathrust events are followed by substantial down-dip creep [*Suwai et al.*, 2004].

[21] **Acknowledgments.** GPS data provided by the ARIA team at JPL and Caltech. All original GEONET RINEX data provided to Caltech by the Geospatial Information Authority (GSI) of Japan. We are grateful to Mariko Sato and Masayuki Fujita for sharing GPS-A data in advance of publication. This paper was improved by the constructive comments of Eric Calais and two anonymous reviewers.

[22] The Editor thanks two anonymous reviewers for their assistance in evaluating this paper.

References

Aoki, Y., and C. H. Scholz (2003), Vertical deformation of the Japanese islands, 1996–1999, *J. Geophys. Res.*, *108*(B5), 2257, doi:10.1029/2002JB002129.

Apel, E. V., R. Bürgmann, G. Steblov, N. Vasilenko, R. King, and A. Prytkov (2006), Independent active microplate tectonics of northeast Asia from GPS velocities and block modeling, *Geophys. Res. Lett.*, *33*, L11303, doi:10.1029/2006GL026077.

Banerjee, P., F. F. Pollitz, and R. Bürgmann (2007), Coseismic slip distributions of the 26 December 2004 Sumatra-Andaman and 28 March 2005 Nias earthquakes from GPS static offsets, *Bull. Seismol. Soc. Am.*, *97*(1A), S86–102.

Hashimoto, C., A. Noda, T. Sagiya, and M. Matsu'ura (2009), Interplate seismogenic zones along the Kuril-Japan trench inferred from GPS data inversion, *Nat. Geosci.*, *2*, 141–144.

Hayes, G. P. (2011), Rapid source characterization of the 03-11-2011 M_w 9.0 off the Pacific Coast of Tohoku earthquake, *Earth Planets Space*, in press.

Heki, K. (2007), Secular, transient and seasonal crustal movements in Japan from a dense GPS array: Implication for plate dynamics in convergent boundaries, in *The Seismogenic Zone of Subduction Thrust Faults*, edited by T. Dixon and C. Moore, pp. 512–539, Columbia Univ. Press, New York.

Herring, T., R. W. King, and S. M. McCluskey (2010), Introduction to GAMIT/GLOBK release 10.4, Mass. Inst. of Technol., Cambridge.

Huang, Z., D. Zhao, and L. Wang (2011), Seismic heterogeneity and anisotropy of the Honshu arc from the Japan Trench to the Japan Sea, *Geophys. J. Int.*, *184*, 1428–1444.

Iinuma, T., M. Ohzono, Y. Ohta, and S. Miura (2011), Coseismic slip distribution of the 2011 off the Pacific coast of Tohoku earthquake (M9.0) estimated based on GPS data—Was the asperity in Miyagi-oki ruptured?, *Earth Planets Space*, in press.

Koper, K. D., A. R. Hutko, T. Lay, C. J. Ammon, and H. Kanamori (2011), Frequency-dependent rupture of the 11 March 2011 M_w 9.0 Tohoku earthquake: Comparison of short-period P wave backprojection images and broadband seismic rupture models, *Earth Planets Space*, in press.

Lay, T., C. J. Ammon, H. Kanamori, L. Xue, and M. J. Kim (2011), Possible large near-trench slip during the great 2011 Tohoku (M_w 9.0) earthquake, *Earth Planets Space*, in press.

Loveless, J. P., and B. J. Meade (2010), Geodetic imaging of plate motions, slip rates, and partitioning of deformation in Japan, *J. Geophys. Res.*, *115*, B02410, doi:10.1029/2008JB006248.

Matsu'ura, T., A. Furusawa, and H. Saomoto (2009), Long-term and short-term vertical velocity profiles across the forearc in the NE Japan subduction zone, *Quat. Res.*, *71*, 227–238.

Miura, S., N. Takahashi, A. Nakanishi, T. Tsuru, S. Kodaira, and Y. Kaneda (2005), Structural characteristics off Miyagi forearc region, the Japan Trench seismogenic zone, deduced from a wide-angle reflection and refraction study, *Tectonophysics*, *407*, 165–188.

Nadeau, R. M., and T. V. McEvilly (1999), Fault slip rates at depth from recurrence intervals of repeating microearthquakes, *Science*, *285*, 718–721.

Nishimura, T., et al. (2000), Distribution of seismic coupling on the subducting plate boundary in northeastern Japan inferred from GPS observations, *Tectonophysics*, *323*, 217–238.

Okada, T., T. Yaginuma, N. Umino, T. Kono, T. Matsuzawa, S. Kita, and A. Hasegawa (2005), The 2005 M7.2 MIYAGI-OKI earthquake, NE Japan: Possible rerupturing of one of asperities that caused the previous M7.4 earthquake, *Geophys. Res. Lett.*,*32*, L24302, doi:10.1029/2005GL024613.

Ozawa, S., T. Nishimura, H. Suito, T. Kobayashi, M. Tobita, and T. Imakiire (2011), Coseismic and postseismic slip of the 2011 magnitude-9 Tohoku-Oki earthquake, *Nature*, *475*, 373–376, doi:10.1038/nature10227.

Pollitz, F. (1996), Coseismic deformation from earthquake faulting on a layered spherical Earth, *Geophys. J. Int.*, *125*, 1–14.

Pollitz, F., P. Segall, and R. Bürgmann (1998), Joint estimation of afterslip rate and postseismic relaxation following the 1989 Loma Prieta earthquake, *J. Geophys. Res.*, *103*, 26,975–26,992.

Pollitz, F. F., et al. (2011), Coseismic slip distribution of the February 27, 2010 Mw 8.8 Maule, Chile earthquake, *Geophys. Res. Lett.*, *38*, L09309, doi:10.1029/2011GL047065.

Sato, M., T. Ishikawa, N. Ujihara, S. Yoshida, M. Fujita, M. Mochizuki, and A. Asada (2011a), Displacement above the hypocenter of the 2011 Tohoku-Oki earthquake, *Science*, doi:10.1126/science.1207401, in press.

Sato, M., H. Saito, T. Ishikawa, Y. Matsumoto, M. Fujita, M. Mochizuki, and A. Asada (2011b), Restoration of interplate locking after the 2005 Off-Miyagi Prefecture earthquake, detected by GPS/acoustic seafloor geodetic observation, *Geophys. Res. Lett.*, *38*, L01312, doi:10.1029/2010GL045689.

Seno, T., T. Sakurai, and S. Stein (1996), Can the Okhotst plate be discriminated from the North American plate?, *J. Geophys. Res.*, *101*, 11,305–11,315.

Simons, M., et al. (2011), The 2011 magnitude 9.0 Tohoku-Oki earthquake: Mosaicking the megathrust from seconds to centuries, *Science*, doi:10.1126/science.1206731, in press.

Suwa, Y., S. Miura, A. Hasegawa, T. Sato, and K. Tachibana (2006), Interplate coupling beneath NE Japan inferred from three-dimensional displacement field, *J. Geophys. Res.*, *111*, B04402, doi:10.1029/2004JB003203.

Suwai, Y., et al. (2004), Transient uplift after a 17th-century earthquake along the Kuril Subduction Zone, *Science*, *106*, 1918–1920.

Suzuki, T. (1989), Late Quaternary crustal movements deduced from marine terraces and active faults, Joban coastal region, northeast Japan, *Geogr. Rep. Tokyo Metrop. Univ.*, *24*, 31–32.

Uchida, N., and T. Matsuzawa (2011), Coupling coefficient, hierarchical structure, and earthquake cycle for the source area of the 2011 Tohoku earthquake inferred from small repeating earthquake data, *Earth Planets Space*, in press.

Uchida, N., J. Nakajima, A. Hasegawa, and T. Matsuzawa (2009), What controls interplate coupling?: Evidence for abrupt change in coupling across a border between two overlying plates in the NE Japan subduction zone, *Earth Planet. Sci.Lett.*, *283*, 111–121.

Ueda, H., M. Ohtake, and H. Sato (2001), Afterslip of the plate interface following the 1978 Miyagi-Oki, Japan, earthquake, as revealed from geodetic measurement data, *Tectonophysics*, *338*, 45–57.

Umino, M., T. Kono, T. Okada, J. Nakajima, T. Matsuzawa, N. Uchida, A. Hasegawa, Y. Tamura, and G. Aoki (2006), Revisiting the three M ~ 7 Miyagi-oki earthquakes in the 1930s: Possible seismogenic slip on asperities that were re-ruptured during the 1978 M = 7.4 Miyagi-oki earthquake, *Earth Planets Space*, *58*, 1587–1592.

Yamanaka, Y., and M. Kikuchi (2004), Asperity map along the subduction zone in northeastern Japan inferred from regional seismic data, *J. Geophys. Res.*, *109*, B07307, doi:10.1029/2003JB002683.

Zhao, D., Z. Wang, N. Umino, and A. Hasegawa (2007), Tomographic imaging outside a seismic network: Application to the northeast Japan arc, *Bull. Seismol. Soc. Am.*, *97*, 1121–1132.

P. Banerjee, Earth Observatory of Singapore, Nanyang Technological University, 50 Nanyang Ave., 639798, Singapore.

R. Bürgmann, Department of Earth and Planetary Sciences, University of California, Berkeley, CA 94720, USA.

F. F. Pollitz, U.S. Geological Survey, 345 Middlefield Rd., MS 977, Menlo Park, CA 94025, USA. (fpollitz@usgs.gov)